

A UNIQUE SINGLE BLADE WIND TURBINE SENIOR DESIGN PROJECT

Steven Walters¹ and Harwood A. Hegna²

¹Honda R&D Americas, Raymond, Ohio; Email: SWalters@oh.hra.com

²Cedarville University, Cedarville, Ohio; Email: hegnah@cedarville.edu

I. Introduction

Is it possible for a single bladed wind turbine to be just as efficient as its multiple bladed counterparts? A Cedarville University senior design team named Zephyr sought to investigate this question by designing, manufacturing, and testing a single blade windmill based on a concept originally introduced by Raymond Holland (1986). This concept uses a single blade with a self-adjusting blade angle of attack and includes multiple degrees of freedom in the blade and body which reduce the stresses and extend the wind turbine's life. The team consisted of four senior mechanical engineering students who had to bring structural analysis, aerodynamics analysis, instrumentation, data collection, and manufacturing together. The prototype was successfully tested to provide insight into the capabilities and difficulties of this innovative design. They experienced many opportunities to practice communication and team building skills throughout the year.

The traditional use of windmills has been to pump water. However, in recent years, wind turbines have been used as a "first step" to bring electrical power to remote areas. Nations such as China, Bangladesh, and many African countries are using small wind turbines to improve the living conditions of their people. Stand-alone, small wind turbines output approximately one thousand Watts, have a blade radius of about 2.5 meters, and cost a few thousand dollars. Their output is DC and use a battery for storage. Most wind turbines today have three rigid blades. Efficiency is limited in wind power as proved by Betz in a calculus derivation. According to the Betz limit, a theoretical windmill with an infinite number of blades has a maximum efficiency of 59.3 percent. The best real life efficiency is around fifty percent. Excellent small windmill efficiency is about thirty percent (Gipe, 1993 and Hunt, 1981). Efficiency is defined as the ratio of the mechanical shaft power to the available wind power and is given by

$$\text{Power} = \frac{1}{2} \rho A_D V^3 \quad (1)$$

where A_D is the maximum swept area of the rotor (un-teetered), V is the free stream velocity of the wind, and ρ is the density of the air. The nacelle, or body, of the wind turbine typically houses the shaft, gearbox, high-speed shaft, mechanical stop, generator, and cooling system. On large turbines, blades are now well over 100 feet long. Because of turbulence from trees, buildings, and the earth, the minimum height for a small turbine body is thirty feet; but for a large turbine, it may exceed over 200 feet. Most small wind turbines have a cut-in speed of about ten to fifteen miles per hour which means they will not operate below that speed.

Mr. Holland sought a fresh approach to wind power when he patented the multiple-axes, free-pivoting windmill concept. Holland's unique windmill design originated from his

American Society for Engineering Education

March 31-April 1, 2006 – Indiana University Purdue University Fort Wayne (IPFW)

2006 Illinois-Indiana and North Central Joint Section Conference

observation of a falling maple seed. When a maple seed drops to the ground, its shape balances itself between the seed and fin. Thus, the fin spins around a central axis, and the maple seed slowly whirls to the ground. Holland supposed that a single blade could be designed to spin around a mill shaft in a similar fashion with the same aerodynamic advantages. Holland believed, “The ability to yield to gusts and to change pitch automatically in response to changed conditions is dynamically inherent in both the maple seed and the free wind turbine blade”. The pitch is critical in Holland’s concept simply because it allows the orientation of the blade, angle of attack, to shift and be in the optimal position for lift throughout the rotation of the blade. Holland intended to make his windmill free of “springiness,” which results from the wind force elastically deflecting the components of a rigid windmill. He recognized that stresses were caused by deflections, which would tend to shorten the structural life. He tried to lessen stresses by means of pivoted joints between parts and the use of ‘soft,’ relatively constant, and smoothly varying centrifugal and gyroscopic moments produced by relative rotations. The windmill parts were to govern smoothly but instantly and firmly in varying wind conditions.

In Fig. 1 Holland denotes the four pivots with P, q, Y, and T. The first four pivots freely rotate through an operating range of angles. The torque resistance of the generator (needed for power production), restrains the mill axis, which is the fifth pivot. Axes P, q, Y, and T represent the blade pitch, body pitch, body yaw, and blade teeter, respectively. The rotation around axis Y without any mechanical stops, or *yawing*, allows the blade and body to rotate into or away from the direction of the wind. The free rotation of the blade about axis P allows the *blade pitch* to adjust to its optimum angle for a given resultant wind velocity, which yields the most lift. The *body pitch axis q* compensates for vertical wind gusts. The T axis allows for the blade to *teeter*, or feather back, when subject to high-speed winds. The purpose of all these axes is to reduce the stresses that occur because of varying wind speed and direction.

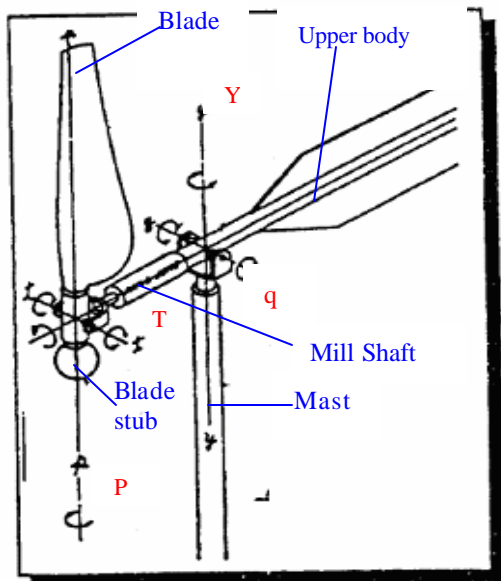


Figure 1. The Axes of Rotation on the Holland Free Pivoting Windmill

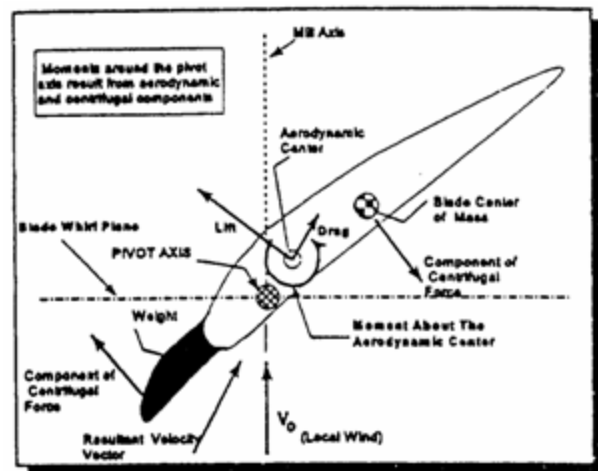


Figure 2. A Sketch of Moments and Forces on a Counterbalance Blade

Figure 2 illustrates the different forces and moments generated while in rotation. Aerodynamically, the blade's properties produce a moment around its aerodynamic center as the blade responds to local wind. With the blade supported on the pitch axis P (located at a defined position ahead of the mean aerodynamic center), the blade's lift and drag also create moments around this axis. Since the blade is free to rotate about the pitch axis, a centrifugal weight is added to the blade to accomplish two functions: first, it statically balances the blade; and second, when in motion, its tendency is to move toward the whirl plane. The second force of the couple is the mass of the blade, acting at the blade's center of mass and located behind the pivot axis. These centrifugal forces cause a moment that balances the effect of the aerodynamic forces for a specific, defined operating condition. Similarly, a weighted stub, located opposite the blade, balances the blade assembly. While in motion, a component of the centrifugal force acting on the stub brings the weight into the whirl plane, thus keeping the blade at the desired teeter angle.

The University of Tennessee Center for Space Transportation and Applied Research (UTCSTAR) first investigated Mr. Holland's concept. They built a sixty percent scale model. They constructed a blade with an attached counterweight and a wooden body with fins that contained the generator, an automobile alternator. They attached the windmill body to a makeshift test stand and observed severe startup problems. Lack of funding terminated their early work. Mr. Holland's heirs arranged with UTCSTAR to give the original model to Cedarville University.

II. Design Considerations

The final design and results presented in this paper represent the culmination of work accomplished by three senior design teams (Bailey, et al, 2002; Bowers, et al, 2003; Walters, et al, 2005). The goal was the design and testing of a windmill system that implemented Mr. Holland's patented design concept. The UTCSTAR blade was the only original component (although modified) used in our design. The first step to design the windmill was to analyze the forces on the blade. The blade begins in static balance which allows the assembly to begin rotation at low wind speeds.

The blade has a NACA 4412 airfoil section constructed with a 30.6 degree twist. The chord varies linearly from 18 inches at the root to 10.8 inches at the tip. The blade root is located one foot from the center of rotation of the mill shaft. The zero lift line for this type of airfoil is at -3.5 degrees for a wide range of Reynolds numbers. The complex nature of the blade presented our senior design group with its first major challenge. In order to analyze the forces on the blade, we implemented our problem solving skills and worked together to break the blade down into simpler components that we could analyze. The blade was numerically divided into one inch segments to estimate the total force on the blade by summing the lift forces acting on each segment using airfoil section characteristics (Abbott, et al, 1959). The incoming wind speed and the rotational speed about the mill shaft were varied to obtain various resultant velocities used in the calculations. The location of the resultant aerodynamic force acting on the entire blade was also estimated.

The blade shaft was redesigned to prevent yielding during normal operation and when the brakes were applied. Both fast and slow stop braking conditions were analyzed. A sudden stop had caused yielding in the original shaft. We assumed that the blade assembly would stop in one second; the wall thickness would be a common size of one-eighth of an inch thick; the outer radius of the shaft would not exceed 1 inch since the blade was not thick enough to contain a 2 inch diameter shaft; the mass of the blade and shaft were point masses; and that only bending occurred. With these assumptions, we were able to write an analysis program. We input the outer radius, the forces, and the rotational speed; and our outputs were the stresses at two points located at the center of rotation and 90 degrees apart. These two points were our concern areas for yielding.

We started with the basic static equations, sum of forces and sum of moments, to find the forces acting on the shaft. We used the static equations because of our assumption that the blade stopped in one second; therefore the blade is in static equilibrium with large stresses at its center of rotation. We also had to calculate the mass moment of inertia, the area of the shaft, and the area moment of inertia. The mass moment of inertia is needed to find the moment caused by the moving blade when it is being slowed down. It is the moment caused by its want to continue to be in motion. Equation 2 is the mass moment of inertia equation. The variables are the mass moment of inertia (I_x), weight of the blade (W_{blade}), the length of the blade (L_{blade}), gravity (g), distance to the center of mass of the blade (d_{cmb}), weight of the shaft (W_{shaft}), length of the shaft (L_{shaft}), and inner radius (r_i).

$$I_x = \frac{W_{blade}}{g} * L_{blade}^2 + \frac{W_{blade}}{g} * d_{cmb}^2 + \frac{W_{shaft}}{g} * L_{shaft}^2 + \frac{W_{shaft}}{2g} * r_i^2 + \frac{W_{shaft}}{g} * \left(\frac{L_{shaft}}{2} \right)^2 \quad (2)$$

Equation 3 gives the calculation of the bending moment by the slowing of a moving object. The variables are the moment (M_{hg}), the mass moment of inertia (I_x), and the rotational speed (rad/sec) (?).

$$M_{hg} = I_x * w \quad (3)$$

Moments were summed to get one final moment in each direction (M_{ty} or M_{tx}). The bending stress was calculated using Eq. 4. The variables in this equation are normal stress in the z direction at point A (s_{za}), moment in the y-direction (M_{ty}), outer radius (r_o), centrifugal force (F_c), area moment of inertia (I_{xx}), and area (A).

$$s_{za} = \frac{M_{ty} * r_o}{I_{xx}} + \frac{F_c}{A} \quad (4)$$

We concluded that we could not have a shaft fit our weight and blade size constraints and stop it suddenly because yielding would occur.

For the more gradual stop, we estimated the brake moment applied to the assembly; assumed the mass of the blade and shaft were point masses; and chose a safety factor of 2, a wall thickness of 0.125 in, and the shaft weight of 9 lbs. The final designed shaft has a diameter of 1.125 in, a wall thickness of 0.125 inch, a weight of 9.2 lbs, and a yield strength of over 66.7 ksi. This blade shaft did not yield during the operational testing which included many controlled, several second stops.

Attaching the blade to our newly designed blade shaft posed a significant problem which caused much debate amongst the team. From testing done by previous senior design teams the blade was severely damaged. Some members of the team thought the blade was so structurally compromised that it would not be able to be repaired for additional testing. A group decision was made to follow one of the team member's idea for repairing the blade and at the same time create a 3D model of the blade that could be used by a machine shop to recreate the blade if necessary. The blade was attached to the redesigned blade shaft using a new "end caps" design. The original blade design had wood ends that added rigidity. We decided to permanently place the end caps inside the fiber glass to reduce the weathering on the end cap material and the blade itself. The end caps are made from a one inch thick fiber glass composite board and a one-eighth inch steel plate bolted together. They are placed inside the blade ends with layers of fiber glass applied over the blade and end caps. Figure 3 shows an end cap placed in the blade with the first layer of fiber glass laid over it and the finished product. We then welded one-half of a collar clamp to each metal end cap. We only welded half of the collar clamp so that it would function properly and attach the blade to the blade shaft. This gave a strong rigid end which could

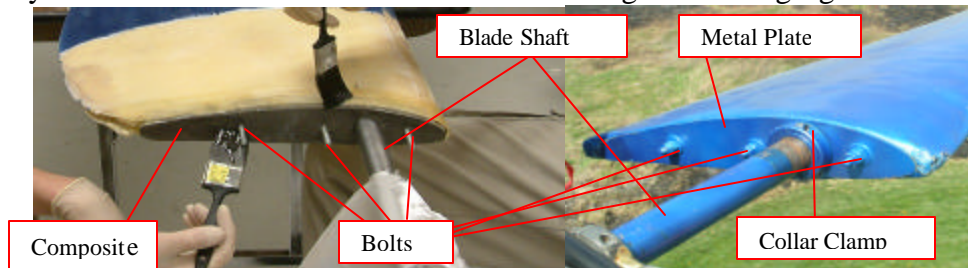


Figure 3. End cap during manufacturing and after completion

transmit the torque when the blade reacts to changes in velocity. The reconstruction of the blade demanded a team effort to finish all of the machining and assembling of parts to make the blade functional again.

The tip end of the shaft has an extended threaded section for easy positioning of a centrifugal weight near the tip. The blade shaft is attached to the interface shaft using roll pins which can withstand over 8000 pounds of centrifugal force. The interface shaft was machined from stainless steel. The bearing housing provides our center of rotation of the blade along with giving the blade its degree of freedom of twisting into the wind. All of the forces from rotation are concentrated at the bearing housing in two bolts that connect it to the yoke.

The windmill frame was constructed with hollow, square cross-section, steel tubing with a vertically mounted shaft using a thrust bearing for smooth rotation on the tower. The vertical fin was aerodynamically sized to direct the windmill into the wind. A wood box nacelle was constructed to cover the generator, drivetrain gearbox, hydraulic disc brake, and associated instrumentation. The sides were hinged for easy access to the components. A Briggs and Stratton E-Tek DC permanent magnet motor served as the generator which was connected to a gearbox with a ratio of 7.63:1. This motor can handle 6 hp at 3100 rpm and 48 volts with 88% efficiency. The body counterweight to balance the turbine assembly is located in the vertical fin part of the frame. The assembled wind turbine is shown in Fig.4.

The early reported severe startup oscillations were designed out by modifying two of the degrees of freedom. The body pitch axis q in Fig. 1 was fixed in the horizontal position. This eliminated some gyroscopic effects. The blade teeter axis T in Fig. 1 was damped after allowing five degrees of motion. The damper system has two variable force dampers that are installed parallel. We set the force in both to about 10 lbs in each direction which is well below the maximum available. The attachment collars for both the mill shaft and the interface shaft were designed to keep the dampers approximately perpendicular to the blade shaft. The collars have aluminum rods bolted between them to help stiffen them. This design, seen in Fig. 5, eliminates torsional shear and keeps the attachments in pure bending.



Figure 4. Wind turbine mounted on tower.

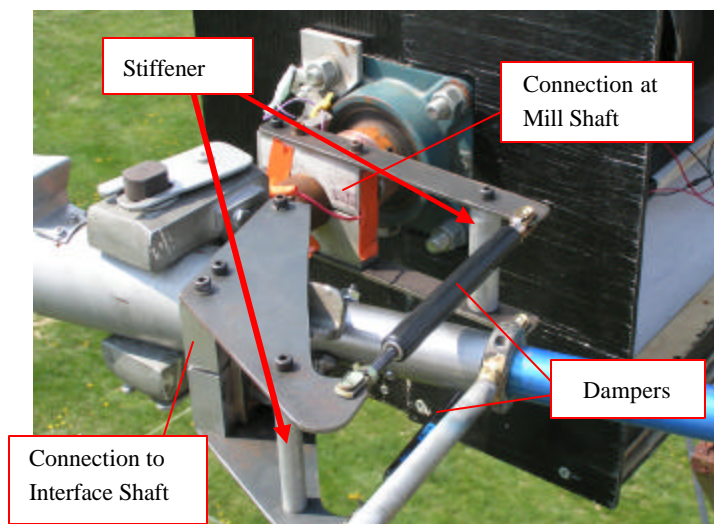


Figure 5. Damper connection.

Instrumentation was designed to measure the blade angle of attack, rotational speed of the mill shaft, power output by the generator, and the free stream wind speed. This data was recorded simultaneously at each time interval. The angle of attack measurement presented special difficulties. The first problem was measuring voltage from an instrument on a spinning blade. We used two copper slip rings attached to the mill shaft with stationary carbide brushes

connected to the frame of the windmill's body as shown in Fig. 6. A radial potentiometer attached to a roller was used to measure the blade angle of attack. The roller moved along the surface of one of the collar clamps by the bearing housing. The potentiometer resistance as a function of rotation angle had a very linear relationship over a 250 degree range. Thus, a limiter was designed to keep the blade angle within broad limits of the potentiometer. The final problem was the actual measurement of the potentiometer voltage. Slip rings may experience a small voltage drop across them. When an instrument measures resistance, it uses a small voltage. If the voltage drop across the rings is greater than this small voltage, then the potentiometer voltage cannot be accurately measured. This problem was solved with a DC voltage divider circuit. Then, the kinematical relation between the potentiometer angle and the blade angle gave the angle of attack based on the voltage drop across the potentiometer.

The small centrifugal weights are a highly experimental aspect and a key element of Mr. Holland's original concept. The weights are each approximately 2 lbs and are threaded onto steel rods. The rods provide easy adjustment of the moment arm length of these weights. The rods are brazed to collar clamps which allow the weights to be placed anywhere along the blade shaft and positioned at different angles. We decided to move the tip weight to a position closer to the center of rotation to lessen the centrifugal forces caused by the rotation about the mill shaft. This modified location would not affect the moment that the weight creates about the pitch axis, but would reduce the moment of inertia generated about the whirl plane. The revised location is shown in Fig. 7. Also seen is the large blade assembly counterweight. It is constructed of several steel plate slices so that the total weight can be easily varied as well as positioned along the shaft.

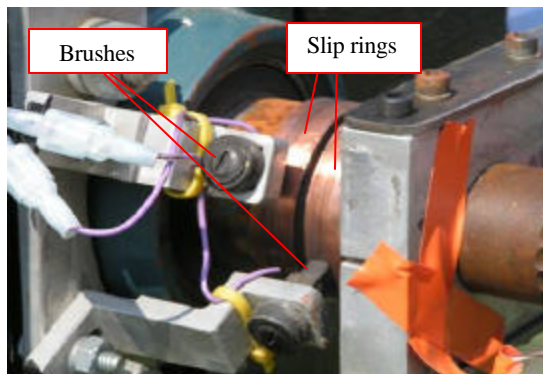


Figure 6. Picture of brushes and slip rings.

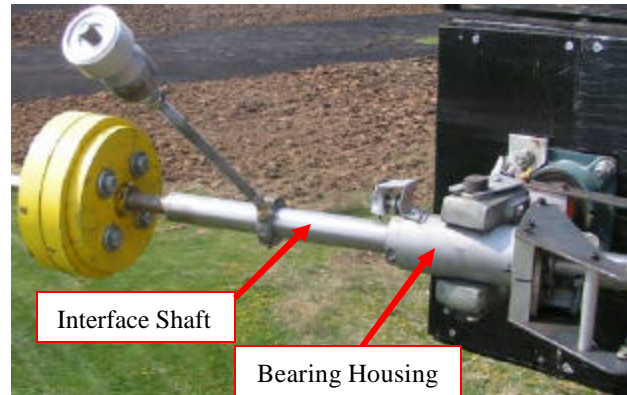


Figure 7. Weight positions.

We found it very difficult to determine the appropriate weight locations for all wind start-up speeds and operating rotational speeds. The only way to determine the proper positioning of the centrifugal weights was experimental. Fortunately with the hard work of the team we were able to finish the construction of the windmill early and had sufficient time to test proper weight locations. Through this testing it was found that in order for the wind turbine to start and achieve high rotational speed, the centrifugal weights had to have an unstable static balance. Unstable static balance means that the blade easily twists out of its initial static balance and into the wind. If the blade is stable, then the blade will not achieve high rotational speed. For the wind

conditions we encountered, the counterweights were positioned to balance the blade to where the root measured angle of attack was between 5 and 10 degrees.

III. Experimental Results

During testing, the variation of the blade angle of attack was demonstrated with the measurements from the potentiometer and slip rings. A sample of the results is shown in Fig. 8. After we released the brake, the blade rotated slowly at about 20 to 25 rpm while the wind speed remained below 13 mph. Near 145 seconds into the test, the wind speed increased and the blade's angle of attack began to adjust automatically. Within about 6 to 8 seconds, the blade angle had increased significantly from 10 degrees to about 60 degrees. The angle of attack is measured between the horizon and the angle of the blade at the root. The self-adjusting blade angle gives the turbine an easier startup while allowing higher efficiencies at greater rotational speeds. This concept is related to the Tip Speed Ratio (TSR) of the blade which is the ratio of the velocity of the blade tip to the velocity of the incoming wind. A lower TSR of 1 to 3 has better starting torque, but a lower efficiency. A higher TSR of 4 to 8 has poorer startup capabilities, but a higher efficiency. On conventional windmills, the blades are designed to operate at a specific TSR that is a compromise between having good starting torque or good efficiency. During startup, our blade had a TSR of less than 2, until the angle of attack increased. At this point, the blade speed accelerated rapidly from about 25 rpm to over 200 rpm in less than 40 seconds. During this interval, the TSR increased from 2 to about 6, thus taking advantage of the better efficiency available at high tip speed ratios. After about 185 seconds, the blade was slowed back down using the brake. As the blade speed decreased, the angle of attack automatically readjusted itself to the startup angle of 10 degrees. These observations

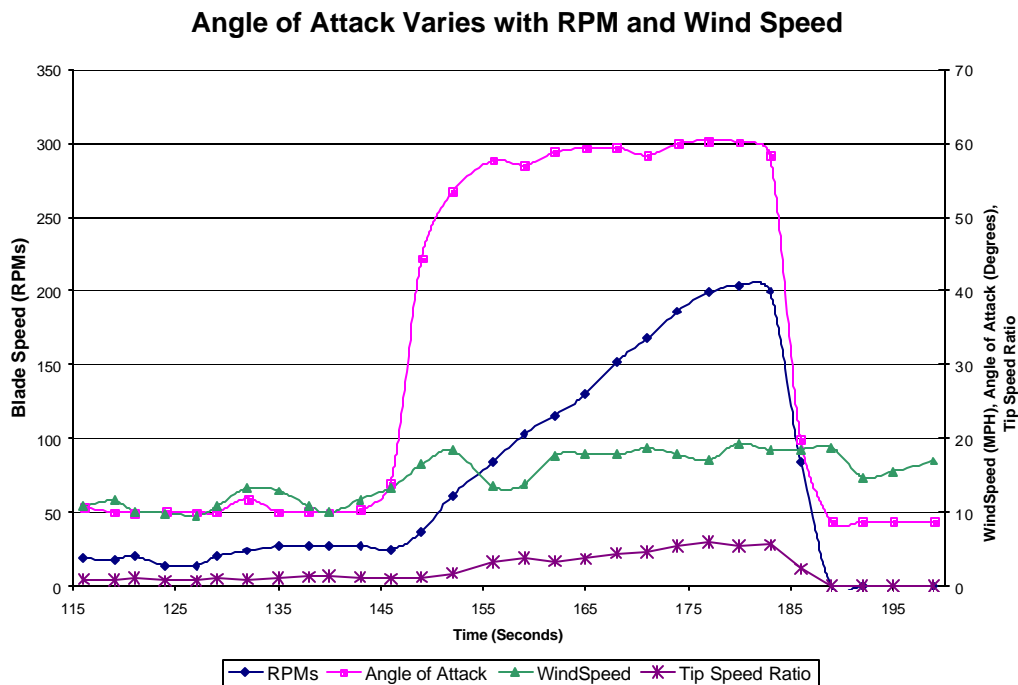


Figure 8. Variation of angle of attack, wind speed, and rotational speed with time .

demonstrate Mr. Holland's theory that the blade could automatically adjust its angle of attack to achieve better torque at startup and readjust for better efficiency while operating.

A power curve plots the power output of a turbine versus the velocity of the wind. Creating a power curve is difficult, however, because the power is not always correlated with the instantaneous speed of the wind. This is because the tiny anemometer can quickly accelerate to match changing winds. However, the heavy blade assembly takes a longer time before it can respond to wind gusts because of its greater inertia. This leads to a lag between wind speed changes and power output. To lessen this discrepancy, we decided to use "wind bins" to create our curve. A wind bin contains wind speeds within a certain interval. For instance, we used one bin to hold all the wind speeds between 5 and 6 mph and another to hold the speeds between 6 and 7 mph. We adjusted the power to account for power lost in the wires. We then took the average of all the power outputs within each bin to make the power curve shown in Fig. 9.

We then compared our experimental power curve with results obtained by Gipe (<http://www.wind-works.org/articles/PowerCurves.html>) for two commercial three-bladed wind turbines. The Bergey Windpower 850, which has a rotor diameter of 8 feet and the Air 403 with 4 foot diameter blades were compared to our windmill with a diameter of 14.4 feet. In 15 mph winds, our turbine produced about 70 watts compared with 200 watts from Bergey and 50 watts from Air 403. In 18 mph winds, our turbine produced about 180 watts compared with 300 watts from Bergey and 100 watts from the Air 403. One interesting thing to note is that at wind speeds between 3 and 7 mph, our single blade turbine is in fact more efficient than the other two windmills. Our turbine has an efficiency between 5 and 14 percent whereas the Bergey 850 and Air 403 have not yet begun to produce power. After 8 mph, however, the efficiencies of the Bergey and Air 403 rapidly increase into the twenties. From this observation, we can conclude that the single blade turbine does, in fact, have a higher efficiency than other comparable wind turbines at low wind speeds (3-8 mph) as predicted by Mr. Holland. We would have liked to do more testing in higher speed winds to find an upper limit to the power output of our wind turbine, but we did not get to test in winds greater than about 20 mph.

IV. Conclusion

A multi-degree of freedom, single blade wind turbine was successfully designed and constructed which implemented Mr. Holland's patented design concept. We were able to take a very complex problem and apply engineering skills and problem solving skill acquired in previous years of study to break the problem down into manageable components. Through cooperative team work we were able to setup and run experiments that would validate the initial design theories. We experimentally demonstrated that the blade's angle of attack changes automatically with the wind speed and blade assembly rotational speed using a system of centrifugal counterweights. This provides for better starting torque at low rotational speeds and greater efficiency at higher speeds. In low wind speeds, this single blade design achieved greater efficiency when compared to similar sized wind turbines. This advantage was lost at higher wind speeds.

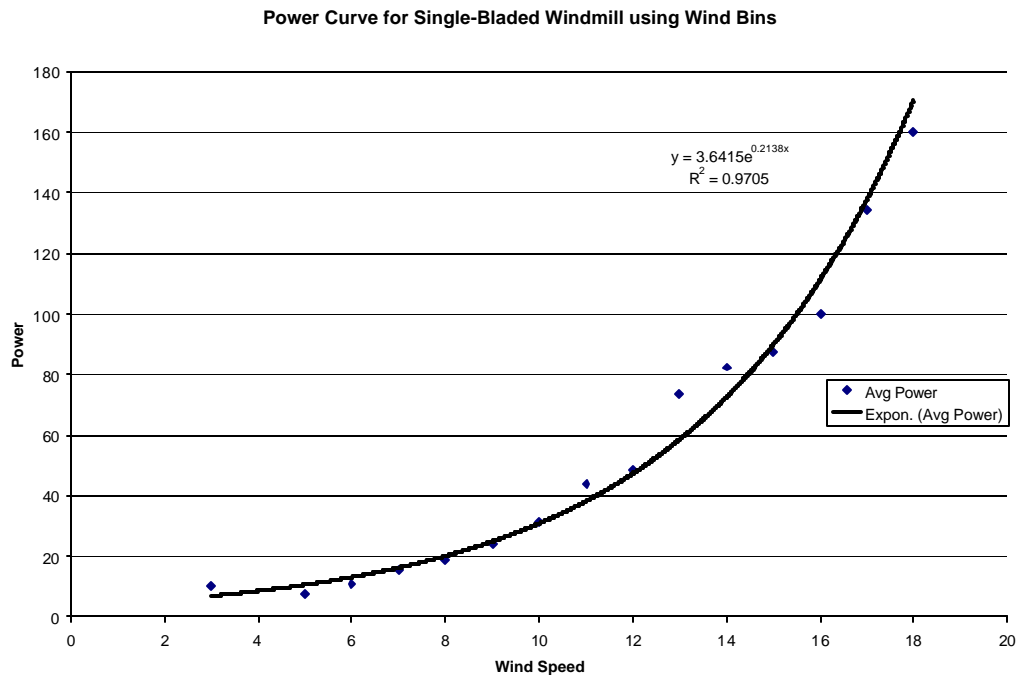


Figure 9. Power curve for single bladed wind turbine using wind bins.

V. Acknowledgments

The authors wish to thank Mr. And Mrs. Steve Nelson for the financial support they provided.

VI. References

- Abbott, I. and Von Doenhoff, A., *Theory of Wing Sections*, Dover, New York, 1959, pp. 488-489.
- Bailey, J., Jenks, W., Mansfield, K., Wakefield, S., *Small, Wind, Free Blade Turbine*, Cedarville University, Dept. of Engineering, 2002, (unpublished).
- Bowers, J., Burke, J., Desatnik, B., Foote, B., Marshall, D., Vargo, A., *A Unique Windmill Prototype for Remote Power Applications*, Cedarville University, Dept. of Engineering, 2003, (unpublished).
- Gipe, P., *Wind Power for Home and Business*, Chelsea Green Publishing, White River Junction, Vermont, 1993, p.62.
- Holland, Jr., Raymond P., "Self Adjusting Wind Power Machine," (United States Patent 4,582,013), U.S. Patent and Trademark Office, Washington, D.C., April 15, 1986.
- Hunt, V. D., *Windpower: A Handbook on Wind Energy Conversion Systems*, Van Nostrand Reinhold Co., New York, 1981, p. 72.
- Walters, S., Sterner, M., Fairbanks, E., Caterinacci, M., *Zephyr*, Cedarville University, Dept. of Engineering, 2005, (unpublished).